Liquid Crystals
Publication details, including instructions for authors and subscription information:
http://www.informaworld.com/smpp/title~content=t713926090

Effect of weak anchoring on the electric field induced deformations of nematic layers

Grzegorz Derfel[a]
[a] Institute of Physics, Technical University of Łódź, Łódź, Poland

To cite this Article Derfel, Grzegorz(1994) 'Effect of weak anchoring on the electric field induced deformations of nematic layers', Liquid Crystals, 17: 3, 429 — 436
To link to this Article: DOI: 10.1080/02678299408036581
URL: http://dx.doi.org/10.1080/02678299408036581

LIQUID CRYSTALS, 1994, VOL. 17, NO. 3, 429–436

Effect of weak anchoring on the electric field induced deformations of nematic layers

by GRZEGORZ DERFEL
Institute of Physics, Technical University of Łódź,
ul. Wólczańska 221, 93-005 Łódź, Poland

(*Received 15 November 1993; accepted 18 February 1994*)

The stationary deformations of nematic layers with a twisted structure are analysed by means of the Taylor expansion method based on catastrophe theory. The role of weak anchoring is investigated. Variations of the polar and azimuthal angles describing the surface director orientation are allowed. The stability of two equilibrium states, the twisted and the homeotropic, is studied. Several types of continuous and discontinuous transitions between them are revealed. The threshold voltages are calculated.

1. Introduction

The finite magnitude of the interaction between a liquid crystal and the electrode surfaces has a significant influence on the behaviour of the liquid crystal electro-optic cell. This influence has been studied in several theoretical publications ([1, 2] and the references cited therein).

In a previous paper [2], a method based on catastrophe theory was applied to this problem. The uniform planar nematic, the twisted nematic and the supertwisted chiral nematic were taken into account. It was assumed, that the director adjacent to the surface could deviate from its initial planar orientation, but did not change its azimuthal angle (i.e. the plane containing the director and the normal to the plates was constant). This is equivalent to the assumption that the infinite surface anchoring energy hindered the director from rotations around the normal to the cell walls, whereas tilt from the surface was allowed, as this deformation was related to the finite energy. Such an approach was also used in earlier studies [3, 4]. It yields remarkable simplifications of the calculations. However, more recent experimental investigations [5, 6] show that the energies of both kinds of anchoring are comparable. Therefore both modes of director deviation should be taken into account. In this paper this more realistic case is treated. The method used is the same as in [2]. It gives qualitative results concerning the stationary states of the system. The ideas involved are briefly mentioned in § 2, where the present problem is formulated and the method of its solution is described. Section 3 contains the results of calculations and some remarks are given in § 4.

2. Method

The idea behind the method applied here is as follows. The free energy of the layer, G, is expressed as a function of the angles which are needed for the qualitative determination of the director distribution. The function G is then reduced to the catastrophe, i.e. to the topologically equivalent function of a standard form. The catastrophe yields a qualitative picture of the behaviour of the layer at small deformations, since it gives the number and disposition of the equilibrium states of the

system in the vicinity of its critical points. The details of the procedure used for the determination of a suitable catastrophe are presented below.

In the system considered, the nematic material, characterized by the elastic constants k_{11}, k_{22} and k_{33}, dielectric permittivities $\varepsilon_\parallel$ and $\varepsilon_\perp$ and intrinsic pitch $P = 2\lambda$, is confined between two electrodes, placed parallel to the (xy) plane at $z = \pm d/2$. The direction of the easy axis at the bottom surface (achieved for instance by rubbing) is twisted in relation to that at the top surface by an angle Φ. The director distribution is determined by the angles $\theta(z)$ and $\omega(z)$ between the director and the (xy) and (yz) planes, respectively. If the deformation are assumed to be small, they can be approximated by their most important Fourier components, and the angles mentioned above, which are

$$\theta(z) = \psi + \xi \cos(\pi z/d), \tag{1}$$

$$\omega(z) = (\Phi - 2\delta)z/d + \chi \sin(2\pi z/d), \tag{2}$$

where ψ is the surface tilt angle, ξ is the amplitude of the small deformation measured in the plane normal to the plates, δ the angle between the easy axis and the projection of the director onto the plates, measured for $z = \pm d/2$, and χ the amplitude of the small deviation from the uniform twist. In this way, the free energy G can be expressed as a function of four variables: $G(\xi\psi\chi\delta)$. The total free energy per unit area of the layer, with respect to an unimportant constant, is given by

$$G = (k_{11}/2)\int_{-d/2}^{d/2}\left[(\cos^2\theta + k_b \sin^2\theta)\left(\frac{\partial\theta}{\partial z}\right)^2 + 2k_t(\pi/\lambda)\cos^2\theta\left(\frac{\partial\omega}{\partial z}\right)\right.$$
$$\left. + \cos^2\theta(k_t\cos^2\theta + k_b\sin^2\theta)\left(\frac{\partial\omega}{\partial z}\right)^2\right]dz$$
$$- \frac{U^2\varepsilon_0\Delta\varepsilon}{2\kappa\displaystyle\int_{-d/2}^{d/2}\frac{dz}{1+\kappa\sin^2\theta}} + 2\gamma_1\sin^2\psi + 2\gamma_2\cos^2\psi\sin^2\delta, \tag{3}$$

where $k_b = k_{33}/k_{11}$, $k_t = k_{22}/k_{11}$, $\kappa = \Delta\varepsilon/\varepsilon_\perp$, $\Delta\varepsilon = \varepsilon_\parallel - \varepsilon_\perp$, U is the applied voltage, γ_1 and γ_2 are the parameters which characterize the strength of the surface anchoring due to the surface tilt and twist, respectively. The expression for the anchoring energy (last two terms in (3)), defines the model potential well for the director bonded with the surface. It is somewhat different from the usual formula $2\gamma_1\sin^2\psi + 2\gamma_2\sin^2\delta$, which is postulated in the literature for small angles. For $\psi = \pi/2$ however, the last expression gives a value which evidently depends on δ, whereas the state $\psi = \pi/2$ is homeotropic and identical for any δ. The modification introduced in (3) allows avoidance of this inconsistency.

The behaviour of the system is investigated in the vicinity of two distinct states corresponding to the critical points of G defined by the set of equations

$$\partial G/\partial\xi = 0, \quad \partial G/\partial\psi = 0, \quad \partial G/\partial\chi = 0, \quad \partial G/\partial\delta = 0. \tag{4}$$

The first critical point, referred to hereafter as the lower point, is due to the undistorted twisted state $\xi = 0$, $\psi = 0$, $\chi = 0$ and $\delta = \delta_1$, where δ_1 is numerically calculated from the minimization condition $\partial G/\partial\delta = 0$

$$k_t[(d/\lambda) + (\phi - 2\delta_1)/\pi] - \gamma_2 d\sin 2\delta_1/k_{11}\pi = 0. \tag{5}$$

The lower critical point is degenerate, i.e. the determinant of the Hesse matrix **H** vanishes for some sets of parameters. The threshold value of the applied voltage is the

most important critical parameter, being the crucial characteristic of the cell. Its value can be found from the equation $\det \mathbf{H} = 0$ for the other fixed parameters. The behaviour of the system in vicinity of the degenerate critical point is given by a suitable catastrophe. In order to determine it, the function $G(\xi\psi\chi\delta)$ is expanded in the Taylor series in the neighbourhood of the critical point

$$G(\xi\psi\chi\delta) = \sum_{ijkl} a_{ijkl}\xi^i\psi^j\chi^k\beta^l \tag{6}$$

where the new variable $\beta = \delta - \delta_1$ was used.

The necessary order of this expansion may be postulated a priori and all the higher order terms appearing during the calculations may be rejected. If the adopted order turns out to be wrong during the final determination of the catastrophe, the whole procedure must be repeated with an increased order of expansion. In this work the calculations were started with the sixth degree, since its correctness was proved for the simpler case in [2].

The transformation of the function of four variables to the catastrophe is rather tedious. In order to shorten the calculations, another approach was applied. The equations

$$\partial G/\partial\chi = 0, \quad \partial G/\partial\beta = 0, \tag{7}$$

where G denotes the truncated Taylor series, determine the functions $\chi(\xi, \psi)$ and $\beta(\xi, \psi)$ in implicit form. This enables one to expand these functions in power series in ξ and ψ in the vicinity of $\xi = 0$ and $\psi = 0$

$$\left.\begin{aligned} \chi(\xi\psi) &= \sum_{ij} p_{ij}\xi^i\psi^j, \\ \beta(\xi\psi) &= \delta - \delta_1 = \sum_{ij} q_{ij}\xi^i\psi^j. \end{aligned}\right\} \tag{8}$$

After the substitution of these series into (6), a function of only two variables is obtained

$$G'(\xi\psi) = \sum_{ij} b_{ij}\xi^i\psi^j. \tag{9}$$

Its values satisfy the condition (7). Therefore its extremes correspond to the extremes of G and the catastrophe equivalent to G can be found without severe difficulties, according to standard procedure given in [7]. This catastrophe describes properly the equilibrium states of the system. By means of a suitable change of variables, the new series is obtained

$$G' = d_{20}w^2 + d_{02}v^2 + d_{04}v^4 + d_{06}v^6 + \ldots, \tag{10}$$

in which w is the inessential variable, and v the essential one. It can be checked by means of numerical examples, that d_{02} and d_{04} can equal zero simultaneously, by a particular choice of parameters, while d_{06} remains different from zero. This justifies the truncation of the series at the sixth degree. It means, that the system is properly described by the butterfly catastrophe.

The second critical point, denoted as the upper, is due to the totally uniform structure aligned normal to the plates. This orientation is sufficiently described by $\xi = 0, \psi = \pi/2$, and the values of χ and δ need not to be specified. This is due to the fact that all the first derivatives of G vanish for arbitrary χ and δ. However the choice of suitable values,

denoted further as χ_2 and δ_2, is necessary, since they are involved in higher order derivatives, i.e. appear in all the coefficients a_{ijkl} of the Taylor expansion

$$G(\xi\phi\chi\delta) = \sum_{ijkl} a_{ijkl}\xi^i\phi^j\eta^k\zeta^l, \tag{11}$$

where the new variables $\phi = \psi - \pi/2$, $\eta = \chi - \chi_2$ and $\zeta = \delta - \delta_2$ were introduced. Before the method of determining χ_2 and δ_2 is described, some properties of the function G, essential for the further procedure, should be mentioned. The values of G for $\xi = 0$, $\psi = \pi/2$, and for arbitrary χ and δ, are equal to zero. This means that G has not any extreme as a function of four variables in the upper state—it is constant with respect to χ and δ. In consequence, no finite Taylor expansion of the function (3) is equivalent to G in the vicinity of this state, and there is no point in transforming it to the form of catastrophe. Obviously, the determinant of the Hesse matrix vanishes, since all the second order partial derivatives, resulting from at least one differentiation with respect to χ or δ, vanish. The critical point $\xi = 0$, $\psi = \pi/2$, $\chi = \chi_2$, $\delta = \delta_2$ is therefore trivially degenerate. The equation $\det \mathbf{H} = 0$ does not define any set of threshold parameters. There is however a possibility of using another function of two variables

$$G'(\xi\phi) = \sum_{ij} c_{ij}\xi^i\psi^j. \tag{12}$$

For this purpose η and ζ are ruled out from (11) by replacing them with functions $\eta(\xi\phi)$ $\zeta(\xi\phi)$

$$\left.\begin{aligned} \eta(\xi\phi) &= \chi - \chi_2 = \sum_{ij} q_{ij}\xi^i\phi^j, \\ \zeta(\xi\phi) &= \delta - \delta_2 = \sum_{ij} p_{ij}\xi^i\phi^j, \end{aligned}\right\} \tag{13}$$

which are found in a way similar to that applied for the lower state, and satisfy the equations

$$\partial G/\partial\eta = 0, \quad \partial G/\partial\zeta = 0. \tag{14}$$

As a result, the extremes of the function G' correspond to the extremes of the function G and therefore to the equilibrium states of the system.

In general, the coefficients c_{ij} resulting from the substitution, are complex combinations of a_{ijkl}. The case $i + j = 2$ is an exception, since the substitution does not affect the second order terms existing in (11). Therefore $c_{ij} = a_{ij00}$ for $i + j = 2$ and the hessian matrix of G' can be constructed by use of the derivatives of the function G. Its determinant is generally different from zero, and the equation $\det \mathbf{H} = 0$ defines the upper threshold voltage U_2. The stability of the critical point $\xi = 0$, $\phi = 0$ changes at U_2, due to the bifurcation which occurs at this point. Therefore close to U_2, other critical points appear for which $\xi \neq 0$, $\phi \neq 0$. They correspond to the critical points of G determined by the equations

$$\partial G/\partial\xi = 0, \quad \partial G/\partial\phi = 0, \quad \partial G/\partial\chi = 0, \quad \partial G/\partial\delta = 0 \tag{15}$$

and characterized by the same values of $\xi \neq 0$ $\phi \neq 0$ and by certain values of $\chi \neq \chi_2$ and $\delta \neq \delta_2$. When U tends to U_2, then the upper state is approached: $\xi \Rightarrow 0$, $\phi \Rightarrow 0$, $\chi \Rightarrow \chi_2$ and $\delta \Rightarrow \delta_2$. Therefore, the set of equations (15), linearized with respect to ξ and ϕ and taken in the limit $\xi \Rightarrow 0$, $\phi \Rightarrow 0$, can be used for calculating values of χ_2 and δ_2. The

number of the equations is reduced by eliminating the electric field. The accessory variable $\alpha = \phi/\xi$ is introduced. The numerical solution of the resulting set of equations gives several sets of χ_2, δ_2 and α, and, in turn, several values of U_2. They determine several possible sequences of the distorted states which may start at $U = U_2$ from the upper state. For this reason the biggest value of U_2 determines the limit of stability of the upper state for $\Delta\varepsilon > 0$, and the smallest U_2 for $\Delta\varepsilon < 0$. The set of χ_2, δ_2 and α corresponding to the properly chosen threshold, should be used in the coefficients a_{ijkl} and c_{ij}. This allows one to determine the catastrophe adequate for description of the behaviour of the system in the neighbourhood of the upper state. By the method sketched previously, the butterfly catastrophe was found.

3. Results

The behaviour of the uniform planar layer is not associated with the strength of the azimuthal anchoring, so the results obtained in the previous paper [2] remain valid. Therefore, only the twisted and supertwisted structures will be described in the following.

The expansion of $G(\xi\psi\chi\delta)$ in Taylor series up to the sixth degree contains 57 and 55 non-zero terms for the lower and the upper critical points, respectively. There is no point in writing them here explicitly.

The strength of the boundary anchoring influences the threshold voltages and the way in which the deformations arise and decay.

The deformations found in the vicinity of the threshold voltages in the lower and upper states are combined together to describe the behaviour of the layer. This is demonstrated in figure 1 by means of the angle $\theta_m = \xi + \psi$, measuring the mid-plane director orientation, plotted against the reduced voltage $u = U^2\varepsilon_0\Delta\varepsilon/\pi^2 k_{11}$ for various sets of other parameters. The left-hand part of each diagram illustrates the behaviour for $\Delta\varepsilon < 0$ and the right-hand part that for $\Delta\varepsilon > 0$. The sets of parameters taken as examples, leading to each of the possible situations, are given in the table. Since all the results are qualitative, only the shapes of the $\theta_m(u)$ dependence are drawn in the figure. Similar curves represent the voltage dependence of the angles ψ χ and δ.

Six relations between the reduced threshold voltages for the lower and upper states can be distinguished: (i) $u_2 > u_1 > 0$, (ii) $u_2 > 0$ and $u_1 < 0$, (iii) $u_1 < u_2 < 0$, (iv) $u_1 > u_2 > 0$, (v) $u_1 > 0$ and $u_2 < 0$, (vi) $u_2 < u_1 < 0$.

The behaviours of the twisted nematic cell ($\Phi = \pi/2$, $d/\lambda = 0$) and of the supertwisted chiral nematic cell ($\Phi/\pi = -d/\lambda$) are similar. Relatively strong anchoring gives the case (i). The transitions may be associated with discontinuities and hystereses as illustrated in figure 1 (*a*)–(*d*). If the anchoring is of medium strength, then case (iv) occurs, which leads to discontinuous switching between the lower and upper states (see figure 1 (*e*)). This effect is more pronounced when $\gamma_2 > \gamma_1$. However for high $\Delta\varepsilon$, deformation of the lower state begins continuously (see figure 1 (*f*)). Figure 1 (*g*) gives the example of continuous deformation of the upper state. For a weak anchoring, two possibilities can be distinguished. If k_b differs significantly from k_t, then case (v) takes place and both states are stable in the absence of the field. Transitions between them are possible given a suitable sign of $\Delta\varepsilon$ and are illustrated in figure 1 (*h*). The upper state is absolutely stable for $\Delta\varepsilon > 0$ and the lower state for $\Delta\varepsilon < 0$. A large twist angle Φ and high elastic anisotropy are conducive to this behaviour. If $k_b \approx k_t$, then case (ii) can be found for a twisted nematic cell. In the absence of the field, the deformed structure is stable. For $\Delta\varepsilon > 0$, the field induces a transition to the homeotropic state, whereas for $\Delta\varepsilon < 0$, the lower state is reached (see figure 1 (*i*)). At very weak anchoring, the

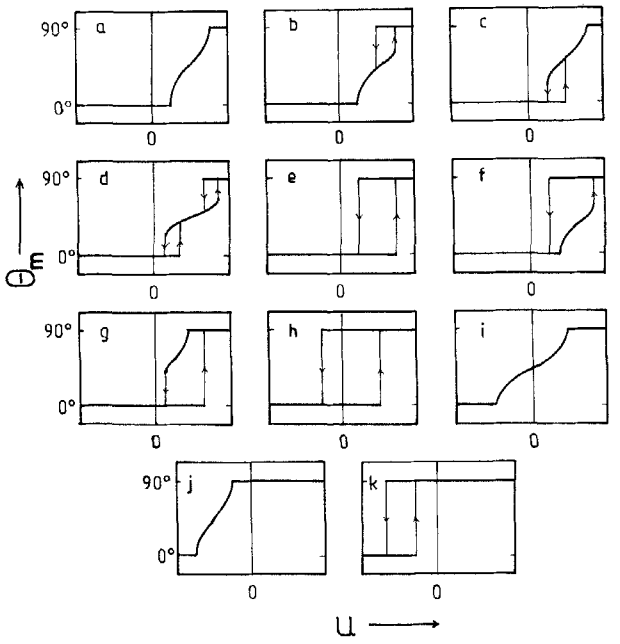

Figure 1. Schematic presentation of the shape of the θ_m (u) dependence showing the stability of the lower and upper states and the possibilities of transitions between them. The sets of parameters used as examples, leading to each situation, are given in the table.

Examples of the parameters leading to various types of behaviour of the nematic cells ($\varepsilon_\perp = 7$, $g_1 = \gamma_1 d/k_{11}$, $g_2 = \gamma_2 d/k_{11}$).

	Twisted nematic cell					Supertwisted nematic cell $\Phi/\pi = -d/\lambda$					
Figure	k_b	k_t	$\Delta\varepsilon$	g_1	g_2	k_b	k_t	$\Delta\varepsilon$	g_1	g_2	Φ/π
1 (*a*)	1·8	0·7	2	10	10	1	0·7	5	10	10	1·5
1 (*b*)	1·8	0·7	2	10	1	1	0·7	10	10	10	1·5
1 (*c*)	1·8	0·7	1	2	20	1·8	0·7	5	10	10	1·5
1 (*d*)	3	0·7	1	2·8	28	1·8	0·7	5	5	5	1·5
1 (*e*)	1·8	0·7	2	0·7	0·7	1·8	0·7	5	2	2	1·5
1 (*f*)	1·8	0·7	20	1	1	1·8	0·7	20	3	3	1
1 (*g*)						1·5	0·4	1	3	30	1
1 (*h*)	1·8	0·7	2, −1	0·5	0·5	1·8	0·7	5, −1	1	10	1·5
1 (*i*)	1	1	5, −1	0·5	5						
1 (*j*)	1	1	−1	0·4	4						
1 (*k*)	1·2	1	−1	0·4	4						

homeotropic state can be stable, without a field, in the twisted nematic cell. Cases (iii) and (vi) are possible as shown in figures 1 (*j*) and (*k*). Transitions in both directions occur for $\Delta\varepsilon < 0$. The situations presented in figures 1 (*i*), (*j*) and (*k*) were not found in supertwisted structures.

The thresholds for the supertwisted nematic cell are plotted versus $g_1 = \gamma_1 d/k_{11}$ in figure 2. The results are presented for three ratios between the two components of the

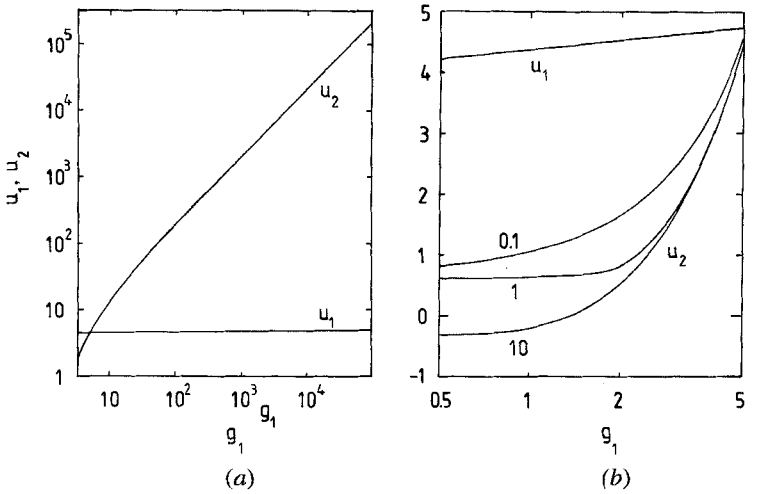

Figure 2 The reduced threshold voltages for the lower and upper states as functions of the anchoring strength $g_1 = \gamma_1 d/k_{11}$, for three γ_2/γ_1 values.

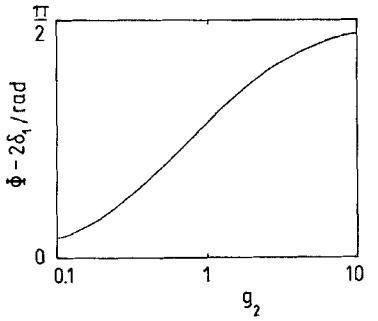

Figure 3. The zero field twist angle $\Phi - 2\delta_1$ for the twisted nematic cell, plotted as a function of $g_2 = \gamma_2 d/k_{11}$.

surface energy: $\gamma_2/\gamma_1 = 10$, $\gamma_2/\gamma_1 = 1$ and $\gamma_2/\gamma_1 = 0{\cdot}1$, which cover the range of diversity of this ratio suggested by experiment [5, 6]. The lower threshold u_1 is independent of γ_2/γ_1 and slightly decreases with decrease of the anchoring strength. The dependence for u_2 is much stronger. The difference between the three γ_2/γ_1 ratios is remarkable only for sufficiently weak anchoring, as shown in figure 2 (*b*). The values of the thresholds do not depend on the dielectric anisotropy $\Delta\varepsilon$. Similar dependences take place for the twisted nematic cell.

If the intrinsic pitch of the chiral material enables the director distribution to fit the easy axes on the plates, i.e. $\Phi/\pi = -d/\lambda$, then $\delta_1 = 0$. In the opposite case, the angle δ_1 differs from zero and therefore the actual twist angle $\Phi - 2\delta_1$ depends on γ_2, as shown in figure 3 for the twisted nematic cell. The curves give only the tendency of the δ_1 variations, since the surface term in expression (3) has a model form.

4. Conclusions

The field effects taking place under weak anchoring circumstances, determined by finite γ_1 but infinite γ_2, were described in [2]. The types of behaviour predicted in the present paper—for finite γ_2—are the same, although the conditions for their occurrence

may differ. The discussion concerning the results obtained in [2] is therefore also valid here. The butterfly catastrophe found for two critical points predicts several means of transitions between them. All the possibilities recognized in [2], are confirmed in the present paper.

To summarize, in nematic twisted structures with typical parameters, the behaviour shown in figure 1 (*a*), (*d*) and (*e*) occurs most often, when weaker and weaker boundary anchoring occurs. The qualitative and stationary character of the solutions shown in figure 1 should be stressed. In particular, the width of the hystereses shown in figures 1 (*b*), (*c*), (*d*), (*f*) and (*g*) cannot be determined precisely, and some types of behaviour may therefore be omitted. On the other hand, the threshold voltages are determined with acceptable quantitative approximation.

In [2], the upper critical point was defined as $\xi = 0$, $\psi = \pi/2$ and $\chi = 0$. The arbitrarily chosen value of $\chi = 0$ is however unjustified. The $\chi_2 \neq 0$ value, found in the manner described in § 2, is proper. Fortunately, this omission has not a great effect on the final results, and the overall picture is the same.

The behaviour described by any catastrophe is valid only in the vicinity of the critical point; in the present problem—for the parameters which are close to those assuring $d_{02} = 0$ and $d_{04} = 0$. In some cases, there is no link between the two $\theta_m(u)$ dependences predicted by the butterfly catastrophe for the upper and lower states. However, one cannot exclude the existence of such a connection sufficiently far from the threshold, where a picture other than that given by the catastrophe may be valid. The approach adopted in the present paper does not give an unequivocal description in such a situation.

It is obvious that the boundary anchoring influences the dynamics of the of the transitions. In particular, the relaxation of the twisted nematic cell, after switching off the electric field, may be rather slow under weak anchoring circumstances. In the case of a chiral material, one may suppose that the action of the intrinsic twist will replace the surface forces.

References

[1] HIRNING, R., FUNK, W., TREBIN, H.-R., SCHMIDT, M., and SCHMIEDEL, H., 1991, *J. appl. Phys.*, **70,** 4211.
[2] DERFEL, G., 1991, *Liq. Crystals*, **10,** 29.
[3] NEHRING, J., KMETZ, A. R., and SCHEFFER, T. J., 1976, *J. appl. Phys.*, **47,** 850.
[4] YANG, K. H., 1983, *J. Phys., Paris*, **44,** 1051.
[5] BLINOV, L. M., KABAYENKOV, A. YU., and SONIN, A. A., 1989, *Liq. Crystals*, **5,** 645.
[6] NOBILI, M., LAZZARI, C., SCHIRONE, A., and FAETTI, S., 1992, *Molec. Crystals liq. Crystals*, **212,** 97.
[7] POSTON, T., and STEWART, I., 1978, *Catastrophe Theory and its Applications* (Pitman).